



Calhoun: The NPS Institutional Archive

Faculty and Researcher Publications

Faculty and Researcher Publications Collection

1991-04-01

Quasimonochromatic x-ray source using photoabsorption-edge transition radiation

Piestrup, M. A.

American Physical Society

Physical Review A, v. 43, no. 7, April 1, 1991, pp.3653-3660
<http://hdl.handle.net/10945/47484>



Calhoun is a project of the Dudley Knox Library at NPS, furthering the precepts and goals of open government and government transparency. All information contained herein has been approved for release by the NPS Public Affairs Officer.

Dudley Knox Library / Naval Postgraduate School
411 Dyer Road / 1 University Circle
Monterey, California USA 93943

<http://www.nps.edu/library>

Quasimonochromatic x-ray source using photoabsorption-edge transition radiation

M. A. Piestrup, D. G. Boyers, C. I. Pincus, and J. L. Harris
Adelphi Technology Inc., 285 Hamilton Avenue, Suite 430, Palo Alto, California 94301

X. K. Maruyama
Naval Postgraduate School, Monterey, California 93943

J. C. Bergstrom, H. S. Caplan, R. M. Silzer, and D. M. Skopik
Saskatchewan Accelerator Laboratory, University of Saskatchewan, Saskatoon, Saskatchewan, Canada S7N 0W0
 (Received 19 November 1990)

By designing transition radiators to emit x rays at the foil material's *K*-, *L*-, or *M*-shell photoabsorption edge, the x-ray spectrum is narrowed. The source is quasimonochromatic, directional, and intense and uses an electron beam whose energy is considerably lower than that needed for synchrotron sources. Depending upon the selection of foil material, the radiation can be produced wherever there is a photoabsorption edge. In this paper we report the results of the measurement of the x-ray spectrum from a transition radiator composed of 10 foils of 2- μm titanium and exposed to low-current, 90.2-MeV electrons. The measured band of emission was from 3.2 to 5 keV. In addition, a measurement was performed of the total power from a transition radiator composed of 18 foils of 2.0- μm copper exposed to a high-average-current electron beam of 40 μA and at energies of 135, 172, and 200 MeV. The maximum measured power was 4.0 mW. The calculated band of emission was from 4 to 9 keV.

I. INTRODUCTION

In a process termed transition radiation, photons throughout the x-ray spectrum are generated when relativistic electrons cross thin foils.¹⁻³ Medium-energy electrons (17–500 MeV) have been shown to generate x rays in the soft⁴⁻⁹ and hard regions of the spectrum.^{10,11} In an earlier work it was noted that the bandwidths of carbon and aluminum transition radiators were narrowed by their *K*-shell photoabsorption edges.⁸ In a more recent work it was shown that using high-density foils such as gold, stainless steel, and copper permits the electron beam to be of moderate energy (100–500 MeV) while still producing warm to hard x rays.^{10,11} Combining these two ideas, one can design transition radiators to emit quasimonochromatically throughout the x-ray spectrum by selection of a material with an appropriate *K*-, *L*-, or *M*-edge frequency.

The bandwidth of the photoabsorption-edge transition radiator can be reduced by a factor of 2 or more when compared to that of a transition radiator which is not designed at the photoabsorption-edge frequency. Since the x-ray absorption is reduced on the low-frequency side of the photoabsorption edge, the number of foils that one can use can be large, permitting intense x-ray production. As an example of this effect at soft-x-ray photon energies, we compare in Fig. 1 the frequency spectra of two transition radiators, one composed of aluminum foils and the other of beryllium. The aluminum radiator spectrum is dramatically truncated above 1.559 keV, while the beryllium's is not. The beryllium stack's *K* edge is at 112 eV and does not affect the spectrum. The absorption of the x rays in the aluminum foils increases by a factor of

10 as the x-ray photon energy passes the *K* edge. This results in the absorption of the x rays with photon energies above 1.559 keV and the abrupt truncation of the frequency spectrum.

II. THEORY

A. Production of transition radiation

When high-energy electrons cross the interface between two media or between a vacuum and a medium, x

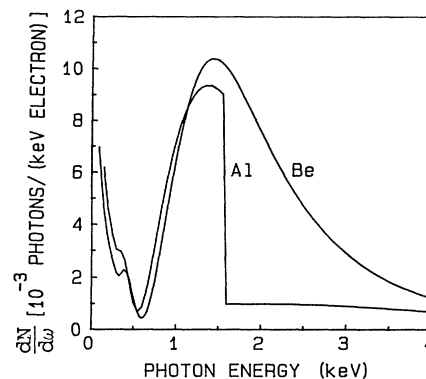


FIG. 1. Calculated effect of *K*-shell photoabsorption edge on the transition-radiation spectrum for 150-MeV electrons. Beryllium has no *K*-shell photoabsorption edge within the energy interval measured here; the aluminum has a *K* edge at 1560 eV. Since there is a large increase in the absorption above the *K* edge, the aluminum spectrum is truncated above 1560 eV.

rays are produced by transition radiation.¹⁻³ The photon production for a single interface is small; however, by stacking a number of foils, the yield can be greatly increased. In most applications, individual foils separated by vacuum are used to reduce reabsorption of the x rays in the medium.

In general, the radiator will be composed of thin foils of thickness l_2 and plasma frequency ω_2 separated by either a gas or vacuum of thickness l_1 and plasma frequency ω_1 (for the gas). For the usual case, when $l_1 \gg l_2$ and $\omega_2 \gg \omega_1$, the radiation is emitted at frequencies less than $\gamma\omega_2$. This frequency represents a "cutoff" frequency above which the radiation falls dramatically.^{6,8,12} Since the plasma frequency of a material is proportional to the square root of its density, this cutoff frequency is proportional to the square root of the foil density.

The spectral intensity produced by a single electron traversing a single-foil interface is given as¹²

$$\frac{d^2N_0}{d\Omega d\omega} = \frac{\alpha\theta^2\omega}{16\pi^2c^2}(z_1 - z_2)^2, \quad (1)$$

where z_1 and z_2 are the formation lengths of two dielectrics given approximately by

$$z_i = \frac{c}{\omega \left[\frac{1}{\gamma^2} + \frac{\omega_i^2}{\omega^2} + \theta^2 \right]}, \quad (2)$$

where $i=1,2$; here θ is the angle of emission with respect to the electron trajectory and ω is the angular frequency of the radiation; ω_i ($i=1,2$) are the plasma frequencies of the two dielectrics; α is the fine-structure constant ($\alpha = \frac{1}{137}$); c is the speed of light; N_0 is the number of generated x-ray photons; Ω is the solid angle in steradians; $\gamma \simeq E/0.511$; and E is the electron-beam energy in MeV.

For the present application, transition x rays are emitted into a narrow forward-directed conical annulus, which at high energies is laserlike in its divergence. The cone half-angle θ is approximately $1/\gamma$, with a width that also is about $1/\gamma$. For 200-MeV electrons, $\theta \simeq \Delta\theta \simeq 2.5$ mrad; thus 4 m from the target the radiation would illuminate an annulus of approximately 6 cm².

For a single electron crossing M foils ($2M$ interfaces), each of thickness l_2 and each separated by a spacing l_1 , the differential production efficiency is¹²

$$\frac{d^2N}{d\Omega d\omega} = \left[\frac{d^2N_0}{d\Omega d\omega} \right] 4 \sin^2 \left[\frac{l_2}{z_2} \right] F(M, X), \quad (3)$$

where

$$F(M, X) = \frac{1 + \exp(-M\sigma) - 2 \exp\left[-\frac{M\sigma}{2}\right] \cos(2MX)}{1 + \exp(-\sigma) - 2 \exp\left[-\frac{\sigma}{2}\right] \cos(2X)}, \quad (4)$$

and $\sigma = \mu_1 l_1 + \mu_2 l_2$, $X = l_1/z_1 + l_2/z_2$, and μ_1 and μ_2 are the linear absorption coefficients of the spacing and foil

media, respectively ($\mu_1 = 0$ for vacuum spacing).

We have numerically integrated Eq. (3) over angle and photon energy to obtain the total power emitted from the radiator. We have used this equation to predict the spectrum for the various radiators discussed in this paper.

The x-ray energy distribution in Eq. (3) combines three basic factors: (a) the single-surface emission modified by (b) the single foil resonance, and (c) the alteration of this band resulting from absorption by downstream foils in the radiator of photons emitted by upstream foils. The second term in Eq. (3), $4 \sin^2(l_2/z_2)$, accounts for coherent or "resonance" addition of amplitudes from the two interfaces of a single foil, and gives a peak value twice as large as from two interfaces when the emission is completely random. This occurs when there is constructive interference between the waves generated at the front and back (upstream and downstream) interfaces.¹²⁻¹⁴ The radiation intensity is maximized when the thickness of the foil is such that both the electron and the photon travel an integral number of wavelengths in the field generated at the first interface. This occurs when $l_2 = (m + \frac{1}{2})\pi z_2$, where m is an integer.

When the intensity varies rapidly with both photon energy and angle, the radiation maxima might be difficult to resolve. These variations are averaged when the detector has low resolution in both solid angle and energy. In addition, the angular distribution is broadened because of both the finite electron-beam dimensions and multiple scattering. When the periods of $F(M, X)$ are not experimentally resolvable and the absorption of the emitted radiation in the foil material is not negligible, Eq. (4) becomes

$$\langle F(M, X) \rangle = \frac{1 - \exp(-M\sigma)}{1 - \exp(-\sigma)}. \quad (5)$$

We see from Eq. (5) that when $M\sigma \gg 2$ the asymptotic value for F is $2/\sigma$, and that beyond $2/\sigma$ foils the radiation intensity cannot be increased significantly by adding more foils. M is approximately 10-24 for the cases presented in Table I. When selecting the maximum number of foils we have used $M = 2/\sigma$ as a rough estimate ($M < 2/\sigma$ for the Sn radiator).

Recently we have shown that by increasing the density of the foils, we can lower the electron-beam energy to moderate values (100-500 MeV).^{10,11} To minimize cost of construction and operation, one wishes the electron-beam energy to be kept as low as possible. By choosing high-density foils, the cutoff frequency $\omega_c = \gamma\omega_2$ is increased. However, since high-density materials often have higher atomic numbers, bremsstrahlung can be large. Hence, in some cases it is important to minimize the bremsstrahlung since it has a flat spectrum from very long wavelengths to photon energies equal to that of the electron-beam energy. Extremely hard x rays are produced for high atomic-number foils which might damage x-ray optics or otherwise be detrimental to other experimental apparatus which is coaxial with the x-ray flux. Thus it is important to select foil materials with thicknesses and densities that minimize the bremsstrahlung and maximize the transition radiation. Selection of materials of high density and moderate atomic number is

TABLE I. Foil stacks designed at their K -edge frequencies.

Material	C	Mg	Al	Ti	Cu	Sn
Density (g/cm ³)	2.3	1.7	2.7	4.5	9.0	7.8
Plasma frequency (eV)	30.6	26.7	32.9	41.4	56.0	52.0
K -absorption edge (keV)	0.28	1.3	1.56	5.0	8.98	29.2
Minimum electron energy (MeV)	5	25	24	61	82	287
Selected electron energy (MeV)	25	75	73	184	244	574
Foil thickness (μm)	0.35	1.9	1.5	3.0	2.9	8.9
Number of foils (M)	10	13	14	18	22	24
Transition-to-bremsstrahlung ratio	5079	507	393	76	33	5

therefore desirable in these situations. For example, iron (stainless steel) and copper foils are excellent candidates since they have comparatively high densities and moderate atomic numbers.

One description of bremsstrahlung that is appropriate for the present purposes assumes relativistic incident electrons and complete screening of the nuclear charge by atomic electrons.¹⁵ In this case the number of bremsstrahlung photons N_B generated by an electron traversing a thickness dl of radiator material can be written

$$\frac{d^2 N_b}{d\omega d\Omega} = N_0 \left[\left(\frac{8\alpha}{\pi\omega} \right) Z^2 r_0^2 \gamma^2 \ln \left(\frac{233}{Z^{1/3}} \right) \frac{1 + \gamma^4 \theta^4}{1 + \gamma^2 \theta^2} \right] dl. \quad (6)$$

N_0 is the number of atoms per cm³ of atomic number Z , and r_0 is the "classical" electron radius ($e^2/mc^2 = 2.8 \times 10^{-13}$ cm). This distribution peaks in the electron-beam direction and has an angular full width of about $1/\gamma$.

Numerically integrating both Eqs. (3) and (6) over a solid angle, we can obtain the ratio of the spectral photon density (photons per unit bandwidth) of transition to bremsstrahlung radiation at photon energies inside the bandwidth of the radiator. The ratio, given for various radiator materials in Table I, can vary widely for different situations: For 1- μm aluminum foils the ratio for 1-keV x rays becomes about 393; but with 8- μm copper foils the ratio for 10-keV x rays becomes about 33. If the ratio is not large, then details of the emissions for both transition radiation and bremsstrahlung must be considered.

B. K -edge transition radiator design

The absorption term in Eq. (4) can include the sudden change in absorption at the photoabsorption edges. The x-ray intensity can be maximized by designing the foil stack at photon energies just below the photoabsorption-edge energy of the foil material. The absorption falls dramatically as the photon energy increases past the K -, L -, or M -edge photon energy. At these edges the absorption can change as much as a factor of 10. A source designed to produce maximum flux at this edge will be quasimonochromatic.

From the requirement that $\omega < \gamma\omega_2$, and given the foil material's K -, L -, or M -edge frequency ω_k and plasma

frequency ω_2 , one picks a minimum electron-beam energy for photon production to be

$$E > \frac{E_0 \omega_k}{\omega_2}. \quad (7)$$

For calculating the foil thickness, an electron-beam energy of between two to six times larger than the minimum energy is selected. The selection is somewhat arbitrary, depending chiefly on the desired x-ray power, since for the energies where $E \gg E_0 \omega_k / \omega_2$, the power radiated is roughly proportional to the electron-beam power.

The single-foil resonance will enhance radiated photons with frequencies that give $l_2 \simeq (\pi/2)z(\omega)$.¹²⁻¹⁴ To enhance the photon production below the photoabsorption edge, we set $\omega = \omega_k$ in Eq. (2):

$$l_2 \simeq \frac{\lambda}{2/\gamma^2 + (\omega_2/\omega_k)^2}. \quad (8)$$

This causes the single-foil resonance term $\sin^2(l_2/z_2)$ in Eq. (3) to be maximum at or near the photoabsorption-edge energy.

From the discussion of Eq. (5) the number of foils is given by

$$M = \frac{2}{\sigma(\omega_k)} = \frac{2}{\mu(\omega_k)l_2(\omega_k)}, \quad (9)$$

where we have again set $\omega = \omega_k$. The mass-absorption coefficients at the photoabsorption-edge energy $\mu(\omega_k)$ were taken from Plechaty, Cullen, and Howerton.¹⁶ One can calculate exact values here, but the values for foil thickness and foil number can vary widely without appreciable change in the radiated frequency spectrum. In fact the parameters used in the experimental section are not optimum.

We have developed a radiator design program using a spread-sheet analysis which follows the design procedure outlined above (see Table I). For a particular electron-beam energy (assuming $E \gg E_0 \omega_k / \omega_2$), foil material, and K -edge frequency, our spread-sheet program will determine foil thickness and number, electron-beam energy, and the ratio of transition to bremsstrahlung radiation. The foil thickness is given by Eq. (8) and the number of foils is given from Eq. (9). For nonresonance (no phase addition between foils) the foil spacing l_1 must be such that $l_1 \gg z_1$. Since z_1 is usually quite small for moderate

electron-beam energies, the spacing is determined by the minimum required thickness of the spacer for rigid support of the foil. The ratio of transition-to-bremsstrahlung radiation was obtained from Eqs. (3) and (6) as described above. Using these electron beam and foil stack parameters as a guide, we can use our computer program to determine the frequency spectrum and angular-emission pattern of the radiator.

Since each element of the periodic chart has different K -, L -, and M -edge frequencies, one can design foil stacks across the x-ray frequency keV band. Using lithium foils we can obtain 55-eV photons, while using gold foils we can obtain 80-keV photons. The calculated spectral power density using a 100- μ A electron beam is plotted in Fig. 2 as a function of x-ray photon energy for four radiators composed of carbon, aluminum, titanium, and tin. Bremsstrahlung radiation is included in the calculation. The spectra are optimized to have peak emission at their respective K -shell photoabsorption edges. Their parameters are given in the figure and in Table I along with other designs for quasimonochromatic radiators which emit across the soft- to hard-x-ray band. Larger fluxes can be obtained by increasing the electron-beam energy or current.

Note there is a large range of foil and electron-beam energy parameters that will permit photoabsorption-edge transition radiation. The values given in Table I are only one set; other values are possible. The designer may be constrained by the electron-beam energy and limited number of available foil thicknesses requiring creative design using the rules outlined above as a guideline.

As an example of hard-x-ray generation, we picked tin foils to produce transition below the tin 29.12-keV K -shell photoabsorption edge (Fig. 2). Such a source would be of value for medical imaging such as digital subtraction angiography where radiation sources are needed on either side of the iodine K edge. The radiator's param-

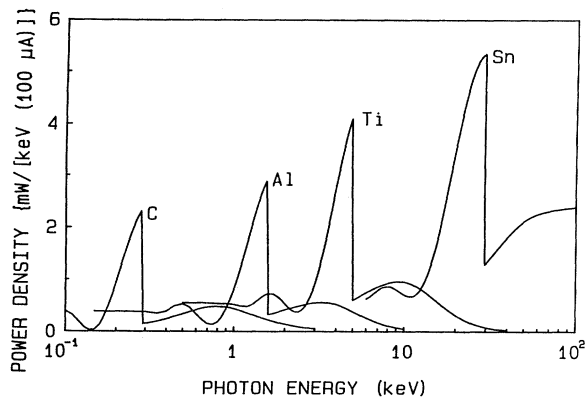


FIG. 2. The spectral power density of four stacks composed of foils of carbon, aluminum, titanium, and tin each optimized at their respective K -shell photoabsorption edges. See Table I. The parameters for the three stacks are C, $E=25$ MeV, $M=10$, $l_2=0.35$ μ m; Al, $E=73$ MeV, $M=14$, $l_2=1.5$ μ m; Ti, $E=184$ MeV, $M=22$, $l_2=2.9$ μ m; and Sn, $E=574$ MeV, $M=24$, $l_2=8.9$ μ m. The average beam current is 100 μ A.

eters are taken from Table I ($M=24$, $l_2=8.9$ μ m, and $E=574$ MeV). The number of foils used is reduced from the $M=2/\sigma$ condition in order to reduce the hard x rays above 29.2 keV. The bandwidth of the tin stack is approximately 40%.

As another example of how the K edge affects the transition-radiation spectrum, we show in Fig. 3, curve (a) the theoretical spectrum of the transition and bremsstrahlung radiation produced by a foil stack composed of 10 foils of 2- μ m titanium (used in the experimental program). This is compared to curve (b), which is the bremsstrahlung and front-and-back-surface transition radiation from a single, equivalent-thickness (20- μ m) titanium foil. Referring to curve (a), at the low-photon-energy end of the spectrum, the photon flux increases with softer photon energies ($\omega < 2.1$ keV); both the transition radiator and the equivalent-thickness single foil have this characteristic soft-x-ray rise. This is due to transition emission from the last-foil interface; the emission from the rest of the interfaces is absorbed in the foils. The flux begins to increase above 2.1 keV because of the rapid drop in x-ray absorption in the foils permitting the x rays produced at each interface to escape. At 4.96 keV there is a sudden drop in the photon flux because of the sudden increase in absorption just above photoabsorption edge energy.

When measuring transition radiation spectra and power, a single foil of thickness equivalent to that of the total foil stack thickness is used to account for the bremsstrahlung and other spurious ionizing radiation from the accelerator. The spectrum from the single foil is subtracted from the spectrum produced from the multiple-foil stack, resulting in a difference spectrum. The difference spectrum gives a somewhat clearer picture of the multiple-foil transition radiation spectrum, especially when there is large spurious radiation coming from sources (e.g., collimators, irises) upstream of the transition radiator. This unfortunately also eliminates the front-and-back-surface transition radiation (TR), which as we can see from Fig. 3(a) is important at soft-x-ray photon energies. The difference spectrum can thus be characterized by the following equation: (multiple-foil TR + bremsstrahlung + spurious radiation) - (bremsstrahlung + front-and-back surface TR + spurious radiation) = difference spectrum. The difference spectrum of Fig. 4 is without the single-interface transition radiation and, therefore, lacks the characteristic rise in the spectrum at soft-x-ray photon energies shown in Fig. 3(a). We have used the difference spectrum to present our data. In the case of the titanium data presented here, the background was relatively low, whereas in the case of the earlier measurements of aluminum and magnesium radiators the background was large. In all three cases we give the subtracted spectra for comparison.

The L or M edge can also be used to make a quasimonochromatic transition radiator in the soft and warm regions of the spectrum. As an example we show in Fig. 5 the calculated spectrum for five foils of 0.31- μ m stainless steel (iron). The electron-beam energy is 150 MeV. The L -edge is at 855 eV; thus the spectrum is from approximately 500 to 855 eV. Stainless-steel foils have been

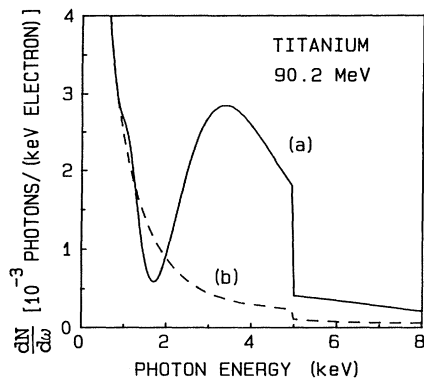


FIG. 3. Predicted spectral photon density for (a) ten foils of 2- μm titanium and (b) and equivalent-thickness (20 μm) single foil of titanium. The electron-beam energy was 90.2 MeV.

used to generate hard x rays and the effect of the K edge at 8.9 keV is apparent in the 400-MeV data.^{10,11}

III. SPECTRA OF ALUMINUM AND MAGNESIUM RADIATORS

Previously, the aluminum and magnesium spectra were measured at the Lawrence Laboratory National Laboratory's Electron-Positron linear accelerator using the experimental setup discussed in Ref. 8. The magnesium spectrum was not published and is presented here for the first time. These low-density foils produced quasi-monochromatic soft x rays. Their spectra are presented here to show the photon-energy shift resulting from their different K -edge photon energies.

The magnesium and aluminum spectra are produced from 54 MeV electrons impinging on the foil stacks at a pulse rate at 1440 s^{-1} . Radiation spectra were measured with a gas-flow proportional counter. All data were measured with a multichannel analyzer. To minimize spectral distortion (pileup), the average number of counts was kept below 0.1 per electron-beam pulse. The required

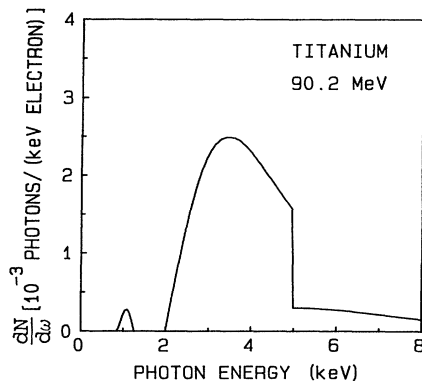


FIG. 4. Predicted spectral photon density of the difference spectrum for ten foils of 2- μm titanium. Spectrum was obtained by subtracting curve (b) from curve (a) in Fig. 3.

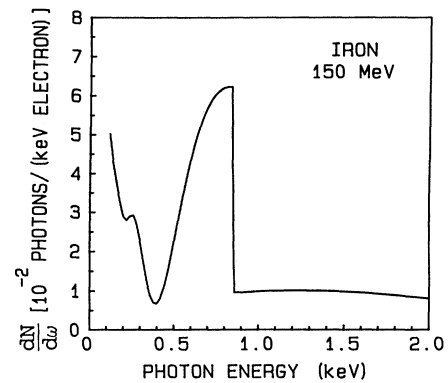


FIG. 5. Predicted spectral photon density from five foils of stainless steel. The radiator has been designed to radiate at the L -shell photoabsorption edge of iron. The electron-beam energy is 150 MeV.

electron-beam current for this count rate was smaller than 1 nA. At this low current level, the absolute beam-current calibration was $\pm 20\%$.

Measured and calculated difference spectra of the magnesium and aluminum stacks are shown in Fig. 6, where

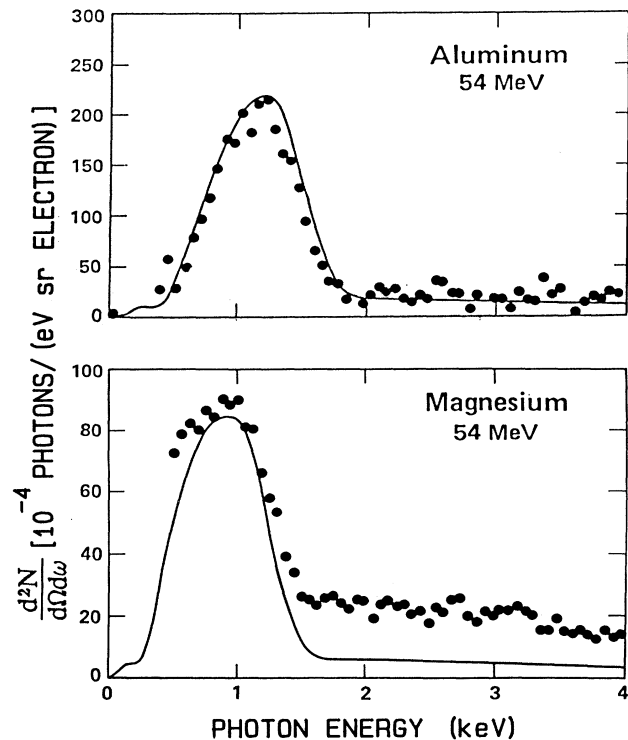


FIG. 6. Measured absolute differential production efficiency of the difference spectrum for the transition radiation emitted from 30 foils of 1- μm magnesium and 30 foils of 1- μm aluminum for the incident electron-beam energy of 54 MeV (from Ref. 8). The magnesium spectrum is truncated at the 1.303-keV K -shell photoabsorption edge. The aluminum is truncated at the 1.559-keV K -shell photoabsorption edge. The truncation of the spectrum is somewhat blurred by the detector frequency resolution.

the number of photons per unit frequency per unit solid angle per electron is plotted as a function of photon energy. Note that due to the method of collection, the units are per solid angle, unlike the other calculated and measured spectra in this paper. These difference spectra have been obtained by subtracting the multiple-foil spectra from the single equivalent-thickness spectra, and hence do not have the characteristic soft-x-ray rise of the radiation from the last-foil interface. The calculated spectra include the effect of the detector resolution (bandwidth). The *K*-edge photon energies of magnesium and aluminum are 1.303 and 1.559 keV, respectively. The sharp falloff of the spectra has been somewhat masked by the bandwidth of the detector. However, the bandwidth-narrowing character of the *K*-edge effect and the shift in the mean frequency between the two spectra are clearly visible.

The measured magnesium-foil spectrum has been raised a factor of 2.8 to match the calculated values. The attenuated output was probably caused by the oxidation of the magnesium foils, which affected either the absorption or photon production. Because of our lack of certainty about this cause, the magnesium spectrum was not included in Ref. 8. However, since the effect of the 1.303-keV *K* edge is evident, the spectrum is included in this paper.

IV. MEASUREMENTS OF A TITANIUM RADIATOR SPECTRUM

The experimental apparatus using the Naval Postgraduate School linear accelerator is shown in Fig. 7. The electron-beam energy was 90.2 MeV. Electrons entered from the left into a vacuum chamber where they passed through the foil stack and then through a dump magnet to be deflected out of the path of the Si-Li detector. The x rays traveled in a 10^{-6} -Torr vacuum before they escaped through a 12.5- μ m Kapton window into the air where they were immediately captured by a Si-Li detector. The detector's peak sensitivity is at 10 keV, and use-

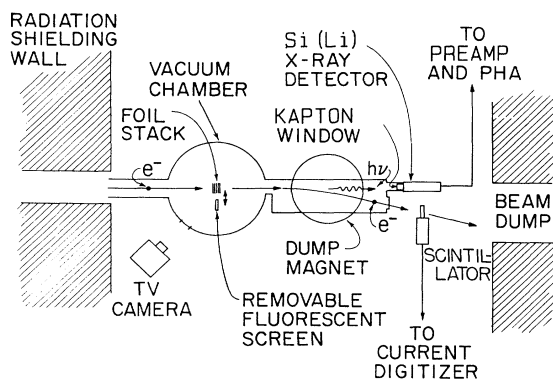


FIG. 7. Diagram of the experimental apparatus to measure hard x rays from a 90.2-MeV electron beam. The distance between the foil stack and the x-ray-detector window is 129 cm. Ten 1- μ m titanium foils were used to produce x rays from 8 to 35 keV.

ful bandwidth, as stated by the manufacturer, is from 1 to 20 keV. Data were gated with the electron-beam spill to reduce the noise background. Electron-beam current was not measured, but the total charge was monitored and kept constant between measurements. At the beginning and end of the experiments a 5894-eV ^{55}Fe x-ray source was used to calibrate the spectra. The detector drift was less than 5% throughout the whole experiment.

The target measured during this experiment was ten foils of 2- μ m titanium. These delicate thin foils were mounted on 1.5-mm-stainless-steel spacers in order to maintain adequate support. Since multiple scattering of the electrons was large, no attempt was made to achieve resonance effects between foils (the condition where there is in-phase addition from one foil to another).

As discussed in Sec. III, a single 28- μ m titanium foil was used to determine the bremsstrahlung and spurious radiation background. The foil was not the same thickness as the total foil stack thickness (20 μ m); however, since the bremsstrahlung generated from the first few microns of the foil is attenuated by the time it has traversed the foil, the difference in power output between the 20- and 28- μ m foils is negligible. The measured radiation generated by the single 28- μ m foil was subtracted from that produced by the foil stack. The spectra from the single 28- μ m foil and the ten foil transition radiator are shown in Fig. 8. No attempt was made to measure the total charge through the foil stack, and thus only the relative intensity was measured. Figure 9 shows the resulting subtracted spectrum. This is to be compared with the theoretical subtracted spectrum shown in Fig. 4.

V. HIGH-CURRENT EXPERIMENT

The experiments were performed at the recently renovated linear accelerator at the Saskatchewan Accelerator Laboratory. This accelerator can produce 50- to 300-MeV electron beams with currents as high as 90 μ A. An existing beamline with a 90° beam dump was available for

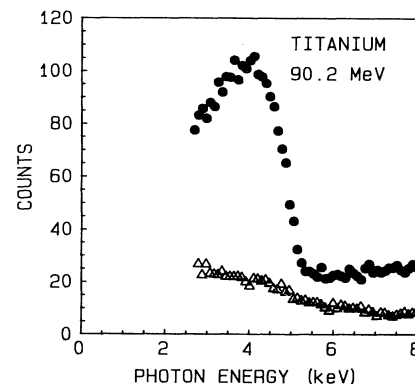


FIG. 8. Measured number of counts for ten 2- μ m titanium foils. The electron-beam energy was 90.2 MeV. The emission from a single 28- μ m foil is also shown. This spectral distribution compares favorably with the calculated spectrum of Fig. 3.

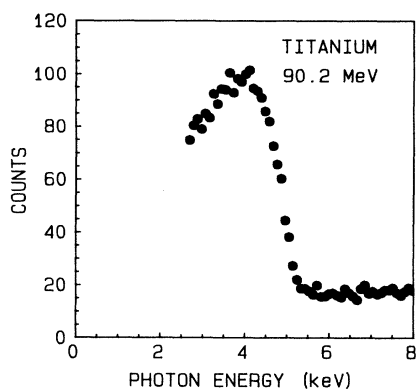


FIG. 9. Relative number of counts from a transition radiator with the equivalent-thickness-foil emission subtracted. The electron-beam energy was 90.2 MeV and the radiator was ten $2\text{-}\mu\text{m}$ foils of titanium. This spectral distribution compares favorably with the calculated spectrum of Fig. 4.

this work. The main components of the experiment were a transition radiator, dump magnet, beam dump, and detector. A side view of the apparatus is shown in Fig. 10. The dump magnet was used to separate the electrons from the x rays. The electrons strike the foil stack, creating the x rays. The electrons are then deflected 90° and dumped into a water-cooled absorber. The x rays then travel 3 m to a planar-diode detector.

The transition radiator consisted of 18 foils of $2\text{-}\mu\text{m}$ copper. The foil diameter was 2.0 cm for adequate electron-beam clearance. A single foil of copper with thickness equivalent to that of the transition radiator ($36\ \mu\text{m}$) was also placed in the electron beam. This allowed comparison of the background radiation due to bremsstrahlung and other ionizing radiation with the transition radiation produced by the copper-foil stack. Since the spectral sensitivity of the photodiode is extremely broadband, the measured bremsstrahlung-background signal was large. The measured signal from the foil stack was

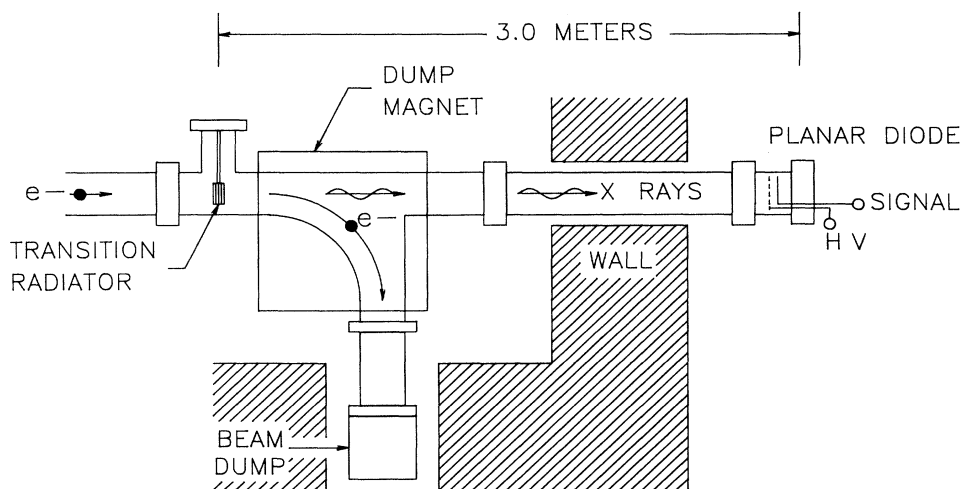


FIG. 10. Diagram of the experimental apparatus to measure the total power of hard-x-ray flux from 18 copper foils each $2.0\ \mu\text{m}$ thick. HV denotes the high-voltage source.

TABLE II. X-ray production from the copper foil stack.

Energy (MeV)	Measured average current (μA)	Estimated theoretical power (mW)	Measured x-ray power (mW)
200	8.6	1.3	1.4
172	40.7	3.6	4.0
135	40.0	2.8	2.5

only a factor of 2 over that of the equivalent foil. Thus only by subtracting the two signals does one get an accurate estimate of the total transition-radiation power.

A phosphor screen, transition radiator, and equivalent-thickness foil were placed in the target holder. The phosphor screen was used to position and focus the electron beam. The foil stack and the equivalent-thickness foil were then translated into the beam for comparison and measurement of the total soft-x-ray power.

To measure the total x-ray flux we utilized an EG&G XRD-41-X planar-diode detector [previously used at Lawrence Livermore National Laboratory (LLNL)].⁹ The photodiode consists of a 74-mm-diam beryllium photocathode plated with $1500\ \text{\AA}$ of aluminum. From Seligson *et al.* we estimated the efficiencies in the bandwidth of the source.¹⁷ Using the measured currents from the diodes and these efficiencies, we obtained the total power generated from the radiator.

Table II gives the x-ray emission that was measured with this arrangement. The measured values agree with the theoretical predictions within experimental error. The maximum power measured was 4 mW. Maximum current through the radiator was $41\ \mu\text{A}$. No unusual cooling scheme was needed for the foils at these currents.

The predicted spectra for the copper radiator are given in Fig. 11 for the three energies used in the experiment. Since the measured spectra for beryllium, aluminum, and titanium have matched their respective calculated ones, Fig. 11 is most likely an accurate prediction.

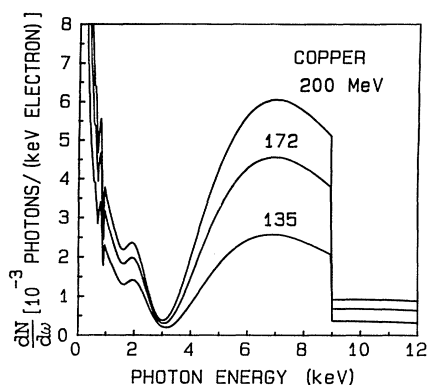


FIG. 11. Calculated spectral photon density for a copper radiator where there is a sudden change in photon production at 8.98 keV due to the *K*-shell photoabsorption edge. The spectrum is given for three energies used in measuring the total power from the radiator.

VI. CONCLUSIONS

We have shown that quasimonochromatic x-rays can be produced from transition radiation using a variety of foil materials as radiators. The source can be designed throughout the soft-, warm-, and hard-x-ray regions of the spectrum with photon energies as low as 55 eV using lithium foils, and as high as 80 keV using gold foils. This radiation is intense, producing milliwatts of power in bandwidths of approximately 50%.

Such a source can offer a relatively inexpensive alternative to synchrotron radiators for many applications. One of the early objectives of the use of synchrotron radiation was to use its inherently pulsed nature combined with its high intensity to permit time-resolved spectroscopy and structural studies. One problem has been that such investigations are feasible only when the electron beam in the storage ring consists of a single, tightly packed bunch of electrons, so that there is time between light pulses to observe the changes in the sample under study. Most synchrotrons operate most easily in a multibunch mode which is so small that the electrons come around the ring too quickly.

Transition radiation offers an alternative to synchrotron radiation for pulsed, high-peak-power production of x rays. The x-ray time structure is controlled by the electron-beam emitter, which can be any of a variety of

medium-energy accelerators such as a linear accelerator, microtron, pelitron, induction accelerator or flash electron source. Each has a unique time structure that may be far more governable or more optimum for a particular experiment than a synchrotron emitter.

Extremely short pulses of x rays can be obtained from transition radiators when used with currently available conventional linacs. Linear accelerators can produce 1-ns- to 10- μ s-long macropulses at a repetition rate of 1–1400 Hz. The macropulse comprises a burst (pulse track) of micropulses. A typical micropulse length is 4–6 ps and a typical micropulse repetition period is 350 ps (760 ps for LLNL). Single micropulses of 2–5 ps have been obtained with millisecond spacing. These single pulses can be on the order of many amperes in peak current. For example, the LLNL electron-positron linear accelerator has a fast-pulse mode in which 12-A electron-beam pulses of between 5 ps and 100 ns can be obtained with millisecond spaces between pulses. We have measured 58-W-peak power in a 17-ns pulse from a soft-x-ray transition radiator.⁹

X-ray pulses with this time structure would be ideal for studying many transient effects in solids and biological materials. The flux for time-resolved x-ray diffraction can be derived from a sequence of one or more micropulses within a single macropulse. If additional flux is required, then one or more macropulses of flux can be employed.¹⁸

ACKNOWLEDGMENTS

The authors would like to acknowledge H. Rietdyk and D. Snyder for their assistance in performing experiments at the linear accelerator facility of The Naval Post Graduate School; also, J. Greefkes and H. Purdy for their assistance in performing experiments at the Saskatchewan Accelerator Laboratory; and G. B. Rothbart for his work in creating the data acquisition and analysis software. The authors would also like to acknowledge the contributions of M. J. Moran, R. H. Pantell, R. K. Klein, B. L. Berman, P. J. Ebert, J. O. Kephart, and H. Park in obtaining the data shown in Fig. 6.⁸ This work was financed by the National Science Foundation of the Small Business Innovative Research (SBIR) program, Grant No. PHY-8460914; the Department of Energy SBIR program, Grant No. DE-FG03-90ER80872; Canadian Natural Science and Engineering Research Council; and the Naval Postgraduate School.

¹V. L. Ginzburg and I. M. Frank, *J. Phys. (USSR)* **9**, 353 (1945).

²G. M. Garibyan, *Zh. Eksp. Teor. Fiz.* **33**, 1403 (1957) [*Sov. Phys.—JETP* **6**, 1079 (1958)].

³M. L. Ter-Mikaelian, *Nucl. Phys.* **24**, 43 (1961).

⁴A. N. Chu, M. A. Piestrup, T. W. Barbee, Jr., and R. H. Pantell, *J. Appl. Phys.* **51**, 1290 (1980).

⁵A. N. Chu, M. A. Piestrup, T. W. Barbee, Jr., R. H. Pantell, and F. R. Buskirk, *Rev. Sci. Instrum.* **51**, 597 (1980).

⁶A. N. Chu, M. A. Piestrup, R. H. Pantell, and F. R. Buskirk, *J.*

Appl. Phys. **52**, 22 (1981).

⁷M. A. Piestrup, P. F. Finman, A. N. Chu, T. W. Barbee, Jr., R. H. Pantell, G. A. Gearhart, and F. R. Buskirk, *IEEE J. Quantum Electron.* **E-19**, 1771 (1983).

⁸M. A. Piestrup, J. O. Kephart, H. Park, R. K. Klein, R. H. Pantell, P. J. Ebert, M. J. Moran, B. A. Dahling, and B. L. Berman, *Phys. Rev. A* **32**, 917 (1985).

⁹M. A. Piestrup and M. J. Moran, *Appl. Phys. Lett.* **50**, 1421 (1990).

- ¹⁰M. A. Piestrup, U.S. Patent No. 4,763,344. (1988).
- ¹¹M. A. Piestrup, M. J. Moran, D. G. Boyers, C. I. Pincus, J. O. Kephart, R. A. Gearhart, X. K. Maruyama, Phys. Rev. A (to be published).
- ¹²M. L. Cherry, G. Hartmen, D. Muller, and T. A. Prince, Phys. Rev. D **10**, 1594 (1974).
- ¹³M. J. Moran, B. A. Dahling, P. J. Ebert, M. A. Piestrup, B. L. Berman, and J. O. Kephart, Phys. Rev. Lett. **57**, 1223 (1986).
- ¹⁴M. A. Piestrup, D. G. Boyers, C. I. Pincus, Qiang Li, M. J. Moran, J. C. Bergstrom, H. S. Caplan, R. M. Silzer, D. M. Skopik, X. K. Maruyama, F. R. Buskirk, J. R. Neighbours, and G. B. Rothbart, Nucl. Instrum. Methods B **40/41**, 965 (1989).
- ¹⁵J. D. Jackson, *Classical Electrodynamics* (Wiley, New York, 1962).
- ¹⁶E. F. Plechaty, D. E. Cullen, and R. J. Howerton, Lawrence Livermore National Laboratory, Report No. UCRL-50400, Vol. 6, Rev. 3, 1981.
- ¹⁷D. Seligion, L. Par, P. King, and P. Pianetta, Nucl. Instrum. Methods A **266**, 612 (1988).
- ¹⁸S. Gruner, Science **23**, 305 (1987).